Available online at www.sciencedirect.com
SCIENCE DIRECT®
Journal of Solid State Chemistry 177 (2004) 189–193
JOURNAL OF SOLID STATE CHEMISTRY
http://elsevier.com/locate/jssc

Selective substitution of alkali cations in mixed alkali glass by solid-state electrochemistry

Kai Kamada,* Yuko Tsutsumi, Shuichi Yamashita, and Yasumichi Matsumoto

Department of Applied Chemistry and Biochemistry, Faculty of Engineering, Kumamoto University, 2-39-1 Kurokami, Kumamoto 860-8555, Japan

Received 26 April 2003; received in revised form 8 July 2003; accepted 12 July 2003

Abstract

Electrosubstitution of alkali cations in mixed-alkali glass containing both Na_2O and K_2O for other monovalent metal cations ($M^+ = Li^+$, Ag^+, and Cs^+) was investigated using a solid-state electrochemical method. The fundamental electrolysis system consists of anode/M^+-conducting microelectrode/glass/Na-β''-Al_2O_3/cathode, where M^+ is substituted for the alkali metal ions in the glass under an applied electric field. Li^+ ions attacked only Na^+ sites, and Ag^+ ions replaced Na^+ sites more readily than K^+. In contrast, Cs^+ ions simultaneously substituted for both Na^+ and K^+ sites. The substitution behavior appears to depend on the difference in ionic conductivity between K^+ and Na^+ and the radius of the dopant. This mechanism was discussed qualitatively.

Keywords: Mixed alkali glass; Electrochemical doping; Microelectrode; Ion exchange; Solid electrolyte

1. Introduction

Functional modification of the glass surface is an effective method of imparting new characteristics to the original glass. Well-established methods for introduction of metal cations into the surface region of glass include the ion-injection technique [1–3] using gas phase ions at low pressure or ion exchange [4–7] using molten salts. The latter technique, usually carried out by immersing the alkali glass into the molten metal salt, is known to be particularly convenient and simple. The alkali ions in the glass are exchanged for the desired metal ions via the concentration gradient across the glass surface. Field-assisted ion exchange has also been performed to accelerate the exchange rate [8,9]. In practice, the introduction of K^+ into sodium silicate glass strengthens the glass [10] and produces refractive index profiles in the glass surface that can be exploited for the preparation of photowaveguides [11]. In general, the characteristics of cation-doped glass strongly depend on the elemental profiles in the glass surface. Thus, many researchers have focused on the relationship between the ion exchange conditions (composition of molten salt, temperature, exchange time) and the elemental distributions in the glass.

We have recently proposed a new solid-state electrochemical route for introducing metal cations into glass using ion-conductors [12]. In this electrochemical approach, an electric field is applied to the solid–solid interface between the cation-conductor and alkali glass, inducing the injection of metal cations (M^{n+}) into the glass and the concurrent substitution of alkali cations in the glass. A significant advantage of this technique is that it enables pinpoint doping into the desired position in the glass with the aid of a β''-Al_2O_3 microelectrode [13–15], owing to which the contact radius of the solid–solid interface is typically about 10 μm.

Until the present study, we mainly employed single-alkali glasses as doping target. In this study, monovalent cations were doped into a glass containing more than one type of alkali ion (mixed alkali glass: MAG) as mobile species by the solid-state electrochemical method as stated above. Surprisingly, the electrosubstitution behavior of alkali ions in MAG changed considerably according to the dopant cation type: The alkali ion type replaced was determined by the dopant type. Greaves et al. has already found an evidence for selective hopping in MAG by using theoretical calculation [16]. Moreover, Bunde et al. mentioned that selectivity depends on the

*Corresponding author. Fax: +81-96-342-3659.
E-mail address: kamada@chem.kumamoto-u.ac.jp (K. Kamada).

0022-4596/$ - see front matter © 2003 Elsevier Inc. All rights reserved.
doi:10.1016/S0022-4596(03)00399-2

mismatch energy, which is an additional energy of A^+ hopping to a B^+ site as compared with A^+–A^+ hopping [17]. Thus, the present experimental study focuses on the electrosubstitution mechanisms for monovalent cation doping (Li^+, Ag^+, and Cs^+) in MAG.

2. Experimental

Electrochemical cation doping was carried out using the experimental setup shown in Fig. 1, where $LiLaSiO_4$, Ag-β''-Al_2O_3, and $CsAlSi_2O_6$ polycrystals were used as Li^+, Ag^+, and Cs^+ conductors, respectively. $LiLaSiO_4$ [18,19] and $CsAlSi_2O_6$ [20] were prepared by a conventional solid-state reaction technique from the corresponding metal oxides and carbonates. The production of these crystalline phases was confirmed by their X-ray powder diffraction patterns. Ag-β''-Al_2O_3 [21,22] was obtained by the ion exchange method using Na-β''-Al_2O_3 pellets in molten $AgNO_3$. To avoid an inhomogeneous current flow, sintered quadrangular microelectrodes were employed as shown in Fig. 1. Assuming a hemispherical microcontact between the microelectrode and glass, the contact radius was typically about 10 μm. A MAG plate ($6Na_2O$–$6K_2O$–$65SiO_2$–$3.5Al_2O_3$–$8B_2O_3$–$6ZnO$–$4TiO_2$ (wt%) and other oxides in trace amounts; thickness: 0.15 mm) was used as doping target. The molar ratio of Na/K in the MAG is calculated to be about 1.7. Cation doping was performed in air under a constant current or voltage with a regulated DC power supply, and at 723 K, i.e., below the glass transition point ($T_g \sim 800$ K). No doping occurred in the absence of an electric field. After doping, the dopant distribution in the cross section of the MAG was measured by electron probe microanalyzer (EPMA, JEOL: JXA8900).

3. Results and discussion

The basic cation migration mechanism in the present system for pinpoint cation doping into glass is illustrated in Fig. 1. Ag anode is electrochemically oxidized to Ag^+ at the Ag/M^+ conductor interface; M^+ is then injected into the glass. Alkali ions (Na^+ and/or K^+) are released from the glass into the cathode side Na-β''-Al_2O_3 for maintenance of electrical neutrality in the glass [23]. Na deposits at the Na-β''-Al_2O_3/Ag (cathode) interface and immediately reacts with ambient O_2 and CO_2 to form Na_2CO_3 [24]. Thus, M^+ is substituted for the alkali ion in the glass under an electric field, hence the use of the term *electrosubstitution* for this doping scheme.

Fig. 2 shows the EPMA elemental distribution maps taken across the cross-sections of three MAG samples doped at 723 K with one of three kinds of monovalent cations (Li^+ (a), Ag^+ (b), and Cs^+ (c)). Only Na and K are indicated in the case of the Li-doped sample because Li cannot be detected by EPMA. The elemental distributions of the other glass forming elements, such as Si, Al, and O, are not affected by electrolysis because the doping was carried out below the T_g. Fig. 2 suggests that the dopant elements (Ag and Cs) were dispersed in the MAG after electrolysis, and that the characteristic X-ray intensity of the alkali ions (Na and K) decreased in the region where dopant was detected. Moreover, alkali ions were detected in the cathode side β''-Al_2O_3 when Ag-β''-Al_2O_3 was used instead of Na-β''-Al_2O_3. These results demonstrate that cation migration as stated above proceeded during electrolysis. We know from our previous studies [13,14] that cation doping results in a hemispherical dopant distribution centered on the microcontact between the ion conductor and glass. In addition, the distribution diameter of the

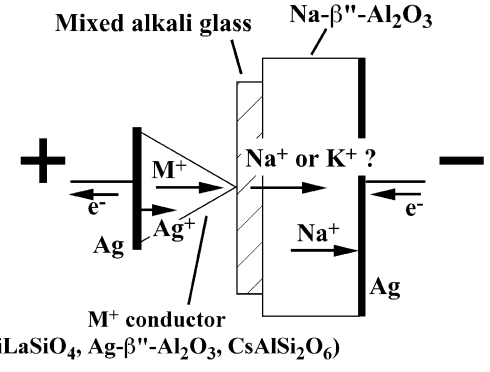

Fig. 1. Model for ion migration in pinpoint cation doping using M^+ ($M^+ = Li^+$, Ag^+, and Cs^+) ion conductors.

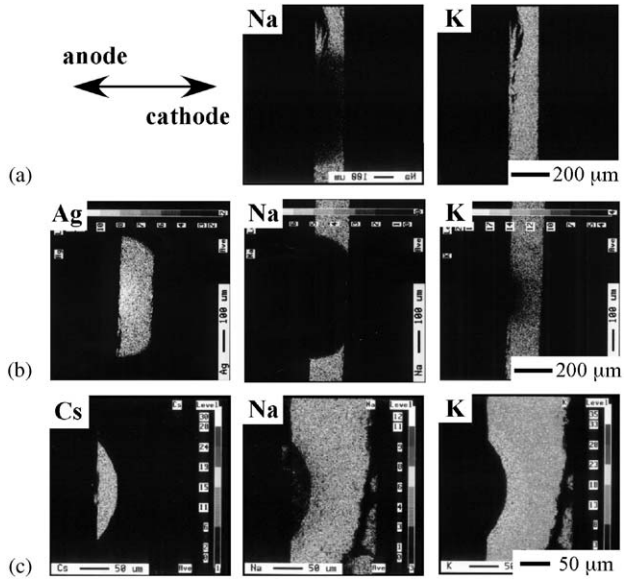

Fig. 2. EPMA elemental distribution maps of the cross-section of the M^+-doped mixed alkali glass by galvanostatic electrolysis at 723 K; (a) Li^+ doping at 10 μA for 60 min, (b) Ag^+ doping at 10 μA for 60 min, and (c) Cs^+ doping at 5 μA for 300 min.

dopant on the anodic surface depended on the current density and/or doping time [25].

The elemental maps of Li-doped MAG (Fig. 2(a)) indicated that Li^+ was doped into the region where the characteristic X-ray intensity of Na was reduced. The occasional cracks observed along the boundary of the doped area may be due to the volume shrinkage in the glass associated with the injection of smaller-sized Li^+ ions. In the case of Li^+ doping (Fig. 2(a)), no electromigration of K^+ ions was observed, while Na was substituted for Li. Thus, in the presence of an electric field, Li^+ selectively attacked Na^+ sites. This result also suggests that a network, in which the only migrating ion is Na^+, forms in the MAG. On the other hand, while Ag^+ mainly replaced Na^+ sites in MAG, a small number of K^+ ions did migrate to the cathode side near the microcontacts (Fig. 2(b)). In fact, the Ag concentration increased in the regions where K was released.

In our previous study, we demonstrated that the Faraday efficiencies of Ag^+ doping into sodium borate glass are above 90% [25]. The doping amount of metal cation was estimated with an ICP spectrometer after dissolving the Ag-doped glass in aqueous HNO_3 solution, and then the current efficiencies were calculated by the relationships between theoretical and measured amounts of Ag using Faraday's law. Consequently, we expected that the Ag-doping into the MAG in this study also proceeded quantitatively under high current efficiency. As shown in Figs. 2(a) and (b), the distribution area of dopant, which reflects the extent of doping was almost the same in the case of Li^+ and Ag^+ doping (10 μA, for 60 min). Thus, cation migration through the solid electrochemical cell was found to proceed readily during Li^+ and Ag^+ doping into the MAG. The distribution area of Cs (Fig. 2(c)) is much smaller than those of the other dopants despite the application of 2.5 times as much electric charge (5 μA for 300 min). A white deposit derived from Cs_2CO_3 was observed on the anodic surface of MAG after Cs^+ doping. These results suggest that the diffusivity of Cs^+ through the glass structure is lower than those of Li^+ and Ag^+. The elemental maps of Cs^+-doped MAG show that the Na and K sites were substituted for Cs^+ to the same extent.

As mentioned above, during solid-state electrochemical cation injection into MAG, the electrosubstitution behavior of alkali ions in the glass, especially that of potassium, is largely governed by the kind of dopant. The mobility of cations in the glass generally depends on the ionic size and electronic structure [26]. The mobility is expected to decrease in the order $Ag^+ > Li^+ > Na^+ > K^+ > Cs^+$ for a given network structure. Since, unlike alkali ions that resemble hard acids, transition metal ions with the d^{10} orbital in their outer shell (Cu^+ and Ag^+) can easily polarize their electron cloud (soft acid), Ag^+ shows a higher ionic conductivity than alkali ions despite being similar in size to Na^+ [27]. Among the alkali ions, ionic conductivity increases with decreasing ionic size. Moreover, the MAG used in the present study contains a larger amount of Na than K (molar ratio of $Na/K = 1.7$). Thus, Na^+ will preferentially migrate in the MAG regardless of dopant type, and will be selectively attacked by dopant cations rather than K^+ [28]. Fig. 2 indicates that the replacement of K^+ in MAG decreases in the order $Cs > Ag > Li$. This may be influenced by the size of the dopant ion, rather than its conductivity. More specifically, the smallest dopant ion, Li^+, substituted only Na^+, which is close to it in ionic size, while the largest dopant ion, Cs^+, replaced both Na^+ and K^+ ions, the former because of its high mobility, the latter because of the similarity of their ionic radii. The other group also suggested that Li^+ can visit to Na^+ site more readily than K^+ site [17]. This fact indicates that the mismatch energy of Li^+ hopping to a Na^+ site will be smaller than that to K^+ site when the Li^+ is obliged to enter a different alkali site.

The applied voltages under constant current during the electrolysis largely differed among the three monovalent dopants (160 V for Ag^+, 130 V for Li^+ doping at 10 μA after 60 min, and 690 V for Cs^+ doping at 5 μA after 300 min). To determine whether electrosubstitution behavior varies with the applied voltage, cation doping was performed under a constant voltage of 1 and 10 V for 600 min at 723 K. The elemental maps of the cross section of the Li^+-doped MAG under constant voltages are shown in Fig. 3. The figure indicates that the Li^+ doping proceeds only at Na^+ sites under different

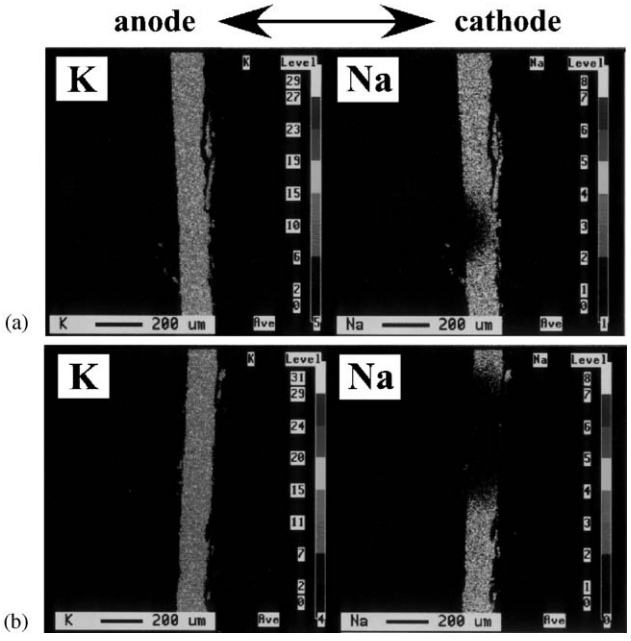

Fig. 3. Elemental maps of the Li^+-doped mixed alkali glass under a constant applied voltage of 1 V (a) and 10 V (b) for 600 min at 723 K.

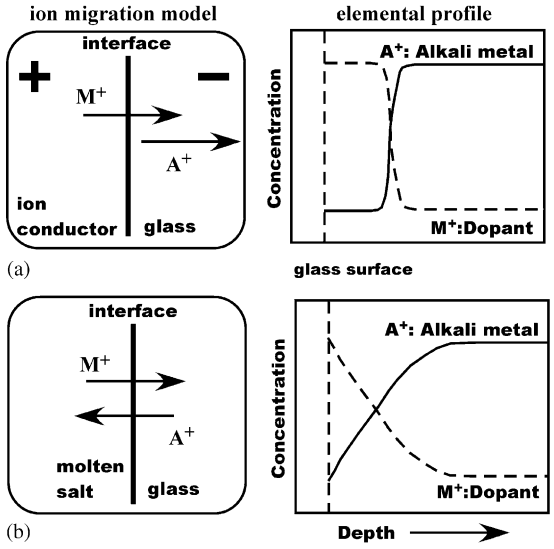

Fig. 4. Schematic models for ion migrations (left hand) and elemental profiles in the glass surface after ion introduction (right hand); (a) solid-state electrochemical technique and (b) ion exchange.

constant voltages, analogous to the doping under galvanostatic conditions. Li injection into the MAG by the ion exchange technique using molten $LiNO_3$ resulted in an equivalent situation in the glass. In the solid-state electrochemical method proposed in this study, the doping occurred by cation diffusion in a single direction from anode to cathode under the applied electric field (Fig. 4(a)) [29]. By contrast, ion exchange proceeds by counter diffusion of dopant and alkali ions across the molten salt/glass interface (Fig. 4(b)). Although the ion migration mechanisms in the two techniques are completely different, the end result of the substitution is similar. Thus, we can conclude that the unique behavior is very sensitive only to the dopant type.

4. Conclusions

In this study, the electrosubstitution behavior of alkali ions (Na^+ or K^+) in the MAG by monovalent cation doping was investigated. It was found that the replaced alkali ion species were determined by the dopant type: the dopant ions selectively replaced Na^+ sites. With larger dopant cation sizes, elimination of K^+ was observed as well. This behavior can be explained by the difference in ionic conductivity and size between the alkali and dopant ions. Fleming and Day [26] reported that Na and K self-diffusion coefficients vary with composition in $(1-x)Na_2O$–xK_2O–$3SiO_2$. Equality of alkali diffusion coefficients (D_K and D_{Na}) under 723 K is observed at $K/(K+Na)=0.78$ depending slightly on the temperature, and D_K is larger (smaller) than D_{Na} above (below) this value. Thus, selectivity of electrosubstitution may be related to not only the dopant kind, but also the framework and the alkali concentration of MAG. One of major differences between conventional ion exchange and the present solid-state electrochemical method is the elemental profiles observed in the glass following dopant introduction. This is because the two methods involve different ion migration mechanisms. As schematically illustrated in Fig. 4, while the concentration profile of the dopant (alkali ion) gradually decreases (increases) with distance from the glass surface in the former method [30], the distribution areas of dopant and alkali ion do not overlap in the case of the latter [29]. However, even when the solid-state electrochemical method is used, a Ag concentration gradient depending on the substitution of K was constructed in the MAG as shown in Fig. 2(b). The graded distribution of dopant is essential for the fabrication of optical devices, such as microlenses and photowaveguides. Therefore, doping experiments involving different cations and glass compositions need to be performed to quantitatively elucidate the selective substitution mechanism.

Acknowledgments

The present work was partly supported by Grant-in-Aid for Scientific Research No. 15760504 from the Ministry of Education, Culture, Science and Technology of Japan. The authors also thank the Asahi Glass Foundation and the Sagawa Foundation for Promotion of Frontier Science for their financial support.

References

[1] G.W. Arnold, J.A. Borders, J. Appl. Phys. 48 (1977) 1488–1496.
[2] H. Hosono, R.A. Weeks, H. Imagawa, R. Zuhr, J. Non-Cryst. Solids 120 (1990) 250–255.
[3] M. Antonello, G.W. Arnold, G. Battaglin, R. Bertoncello, E. Cattaruzza, P. Colombo, G. Mattei, P. Mazzoldi, F. Trivillin, J. Mater. Chem. 8 (1998) 457–461.
[4] H. Hofmeister, S. Thiel, M. Dubiel, E. Schurig, Appl. Phys. Lett. 70 (1997) 1694–1696.
[5] B. Roy, H. Jain, S. Roy, D. Chakravorty, J. Non-Cryst. Solids 222 (1997) 102–112.
[6] M. Dubiel, S. Brunsch, U. Kolb, D. Gutwerk, H. Bertagnolli, J. Non-Cryst. Solids 220 (1997) 30–44.
[7] M.A. Villegas, J.M. Fernàndez Navarro, S.E. Paje, J. Llopis, Phys. Chem. Glasses 37 (1996) 248–253.
[8] M.H. Shaaban, M.K. El Nimr, A.A. Ahmed, J. Mater. Sci.: Mater. Electron. 4 (1993) 208–214.
[9] M.H. Shaaban, A.A. Ahmed, A.R. Cooper, Phys. Chem. Glasses 40 (1999) 34–39.
[10] V.M. Sglavo, D.J. Green, J. Am. Ceram. Soc. 84 (2001) 1832–1838.
[11] J. Kosikova, J. Schrofel, J. Mater. Res. 14 (1999) 3122–3129.
[12] Y. Matsumoto, Solid State Ionics 100 (1997) 165–168.
[13] K. Kamada, S. Udo, Y. Matsumoto, Electrochem. Solid State Lett. 5 (2002) J1–J3.

[14] K. Kamada, S. Udo, S. Yamashita, Y. Matsumoto, Solid State Ionics 146 (2002) 387–392.
[15] K. Kamada, S. Yamashita, Y. Matsumoto, J. Mater. Chem. 13 (2003) 1265–1268.
[16] G.N. Greaves, W. Smith, E. Giulotto, E. Pantos, J. Non-Cryst. Solids 222 (1997) 13–24.
[17] A. Bunde, K. Funke, M.D. Ingram, Solid State Ionics 86–88 (1996) 1311–1317.
[18] H. Matsumoto, K. Yonezawa, H. Iwahara, Solid State Ionics 113–115 (1998) 79–87.
[19] M. Sato, Y. Kono, H. Ueda, K. Uematsu, K. Toda, Solid State Ionics 83 (1996) 249–256.
[20] S. Nakayama, S. Kuwata, T. Ichimori, M. Okazaki, M. Okamasa, S. Imai, M. Sakamoto, Y. Sadaoka, J. Ceram. Soc. Japan 106 (1998) 715–718.
[21] G.S. Rohrer, G.C. Farrington, Chem. Mater. 1 (1989) 438–444.
[22] J.L. Briant, G.C. Farrington, J. Solid State Chem. 33 (1980) 385–390.
[23] C. Thévenin-Annequin, M. Levy, T. Pagnier, Solid State Ionics 80 (1995) 175–179.
[24] Y. Matsumoto, K. Akagami, K. Kamada, J. Solid State Chem. 143 (1999) 111–114.
[25] K. Kamada, S. Udo, S. Yamashita, Y. Tsutsumi, Y. Matsumoto, Solid State Ionics 160 (2003) 389–394.
[26] T. Minami, J. Non-Cryst. Solids 95–96 (1987) 107–118.
[27] M. Tatsumisago, T. Minami, Bull. Ceram. Soc. Japan 29 (1994) 499–501.
[28] J.W. Fleming Jr., D.E. Day, J. Am. Ceram. Soc. 55 (1972) 186–192.
[29] M. Abou-El-Leil, A.R. Cooper, J. Am. Ceram. Soc. 62 (1979) 390–395.
[30] J.M. Inman, S.N. Houde-Walter, B.L. McIntyre, Z.M. Liao, R.S. Parker, V. Simmons, J. Non-Cryst. Solids 194 (1996) 85–92.